

# Methanol oxidation on Fe<sub>2</sub>O<sub>3</sub> catalysts and the effects of surface Mo

M. Bowker,<sup>ab</sup> E. K. Gibson,<sup>\*ac</sup> I. P. Silverwood<sup>ad</sup> and C. Brookes<sup>ab</sup>

Received 15th December 2015, Accepted 22nd December 2015

DOI: 10.1039/c5fd00225g

The adsorption of methanol on haematite has been investigated using temperature programmed methods, combined with *in situ* DRIFTS. Model catalysts based on this material have then been made with a shell–core configuration of molybdenum oxide monolayers on top of the haematite core. These are used as models of industrial iron molybdate catalysts, used to selectively oxidise methanol to formaldehyde, one of the major chemical outlets for methanol. Haematite itself is completely ineffective in this respect since it oxidises it to CO<sub>2</sub> and the DRIFTS shows that this occurs by oxidation of methoxy to formate at around 200 °C. The decomposition behaviour is affected by the absence or presence of oxygen in the gas phase; oxygen destabilises the methoxy and enhances formate production. In contrast, when a monolayer of molybdena is placed onto the surface by incipient wetness, and it remains there after calcination, the pathway to formate production is blocked and formaldehyde is the main gas phase product in TPD after methanol dosing.

## Introduction

This paper concerns the adsorption and reaction of methanol with iron oxide (haematite) and model catalysts of Mo monolayers deposited on that oxide. This is of importance for a variety of reasons. Firstly, iron oxide is one of the most abundant materials readily available on earth and so represents an interesting base material for catalysis from both an economic and environmental point of view. Due to its abundance it is relatively cheap and environmentally cleaner as it is usually mined from near the surface of the earth, therefore little energy is wasted in separation and refining, in contrast to the situation for precious metals. It is also used in a variety of catalytic applications, such as ammonia synthesis, the

<sup>a</sup>UK Catalysis Hub, Research Complex at Harwell (RCAH), Rutherford Appleton Laboratory, Harwell, Oxon, OX11 0FA, UK. E-mail: emma.gibson@rc-harwell.ac.uk

<sup>b</sup>Cardiff Catalysis Institute, School of Chemistry, Cardiff University, Main Building, Park Place, Cardiff, CF10 3AT, UK

<sup>c</sup>Department of Chemistry, University College London, 20 Gordon St., London, WC1H 0AJ, UK

<sup>d</sup>ISIS Neutron and Muon Facility, Science and Technology Facilities Council, Rutherford Appleton Laboratory, Harwell Science and Innovation Campus, Oxon OX11 0QX, UK



high temperature water-gas shift reaction (HTWGS), Fischer–Tropsch synthesis of hydrocarbons and styrene synthesis by ethyl benzene dehydrogenation.<sup>1–4</sup> It must be noted, however, that in the active phase of ammonia synthesis it is in metallic form, in FTS, it is probably carbidic, while in HTWGS, although prepared as haematite, it is in the magnetite form during reaction. However, it is also used as part of the process for the selective oxidation of methanol, which consists of iron in compound form with molybdenum<sup>5</sup> and in its ferric state. In connection with the latter, we are interested in the way in which methanol interacts not only with iron oxide, but as we report below, we have investigated also model methanol oxidation catalysts by placing monolayers of Mo at the surface. We report the changes in behaviour of reactivity and surface species formed when such model catalysts are fabricated using temperature programmed methods and DRIFTS.

## Experimental

The Fe<sub>2</sub>O<sub>3</sub> catalyst used in this study was a commercial Fe<sub>2</sub>O<sub>3</sub> (Sigma-Aldrich, <50 nm particle size). A catalyst of the type MoO<sub>x</sub>/Fe<sub>2</sub>O<sub>3</sub> was synthesised by doping 6 monolayer equivalents of Mo oxide onto the Fe<sub>2</sub>O<sub>3</sub>. The desired amount of aqueous ammonium heptamolybdate was dosed onto the surface of the Fe<sub>2</sub>O<sub>3</sub> by incipient wetness impregnation. The sample was dried at 120 °C for 24 h, before being calcined in a muffle furnace in air at 500 °C, for 24 h.

Reactor data was obtained by use of a CATLAB reactor (Hiden Ltd, Warrington, U.K.). For the catalytic reaction (TPO/TPR), 1 μL of liquid methanol was injected every 2 min into a flow of 10% O<sub>2</sub>/He or He, at a flow rate of 30 mL min<sup>-1</sup>. The products were determined by the online mass spectrometer in the CATLAB system. For the TPD, approximately 6 injections of 1 μL of methanol were dosed onto the catalyst, at ambient temperature in a flow of 30 mL min<sup>-1</sup> of 10% O<sub>2</sub>/He or He. This was followed by ramping the temperature to 400 °C at a rate of 8 °C min<sup>-1</sup>, while monitoring the products formed by mass spectrometry.

*In situ* diffuse reflectance infrared Fourier transform spectroscopy (DRIFTS) was performed in a Harrick high temperature DRIFTS cell fitted with ZnSe windows. The cell was attached to the Praying Mantis Optics and spectra collected with an Agilent Carey 680 FTIR spectrometer, taking 64 scans with a resolution of 4 cm<sup>-1</sup> using the DTGS detector. The TPD and TPO experiments were performed by injecting approximately 5 injections of 1 μL of methanol at ambient pressure in a flow of 30 mL min<sup>-1</sup> of 10% O<sub>2</sub>/He or He. The temperature was then ramped at 10 °C min<sup>-1</sup> while collecting spectra every 15 °C.

## Results and discussion

Fig. 1 shows TPD data from the adsorption of methanol on the iron oxide catalyst. A simple pattern is observed, and is similar to that reported by us previously.<sup>6</sup> That is, weakly held methanol is desorbed at low temperatures, with a maximum at 100 °C. This is then followed by a major desorption at around 300 °C, when both CO<sub>2</sub> and hydrogen desorb, though the line-shapes for the two are a little different. The hydrogen shows a shoulder (at ~250 °C) on the main peak at 300 °C, while the CO<sub>2</sub> appears to be a single peak at ~305 °C. As reported previously<sup>6–8</sup> this desorption is likely to be due to the presence of a formate species on the surface. This is confirmed by the *in situ* TPDRIFT (temperature-programmed diffuse reflectance



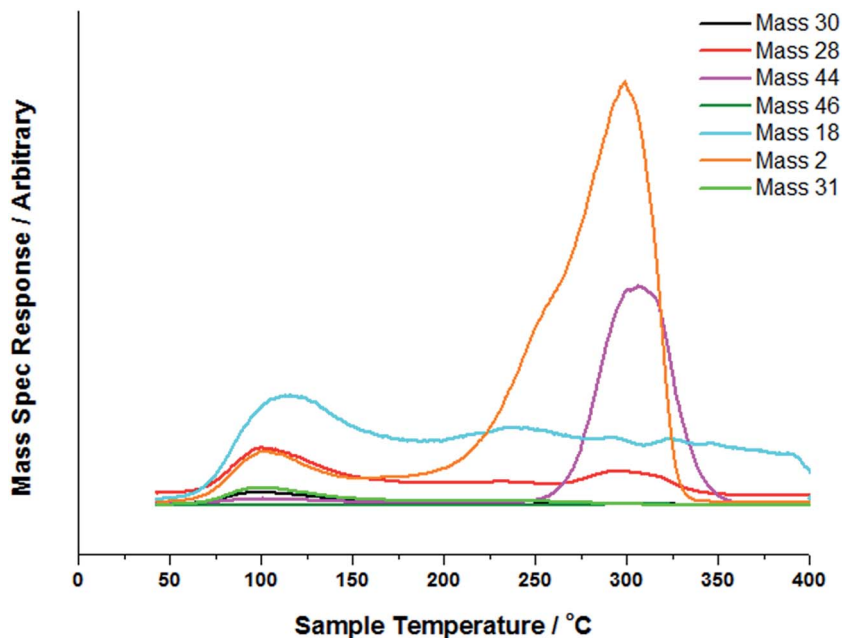


Fig. 1 TPD profile of Fe<sub>2</sub>O<sub>3</sub> under a 8 °C min<sup>-1</sup> ramp in a flow of He after methanol adsorption.

infra-red Fourier transform) spectra in Fig. 2, but additionally here we can identify the temperature range in which the formate is formed. Upon adsorption we see a variety of bands due to a mixture of methanol and methoxy, but after heating to ~100 °C, we are left with just methoxy bands at 1070, 2827 and 2937 cm<sup>-1</sup> (Table 1). Upon heating above about 175 °C, formate bands (1569, 1377, 1358 and 2866 cm<sup>-1</sup>, Table 1 and references therein) start to appear and methoxy is slowly lost, leaving mainly formate at 325 °C. Thus the formate is present on the surface before the desorption of CO<sub>2</sub>, but is not present upon adsorption, so it is formed during the heating process. Most of the hydrogen desorption is clearly from the methoxy decomposition, the methoxy loss rate from the IR data being maximised at ~250 °C (Fig. 3), beginning at ~200 °C and being 80% diminished by 300 °C. Thus it appears that the low temperature shoulder on the hydrogen curve in Fig. 1 is associated with the methoxy decomposition, but the maximum in hydrogen evolution occurs well after most of the methoxy has been lost.

One thing which is immediately obvious from the TPD data is that very little water is evolved from the catalyst during the experiment, and this is unusual for oxidic catalysts: for instance, similar experiments with MoO<sub>3</sub> yield water and no hydrogen ((ref. 6 and 7) and see below). This further implies that hydrogen has difficulty extracting oxygen from the iron oxide lattice in these circumstances, a feature which is an obvious advantage when considering a reaction such as the water-gas shift reaction in the forward direction, eqn (1). Iron oxide is the catalyst for the high temperature shift reaction,<sup>1</sup> though under operating conditions it is thought to be present in the form of magnetite.



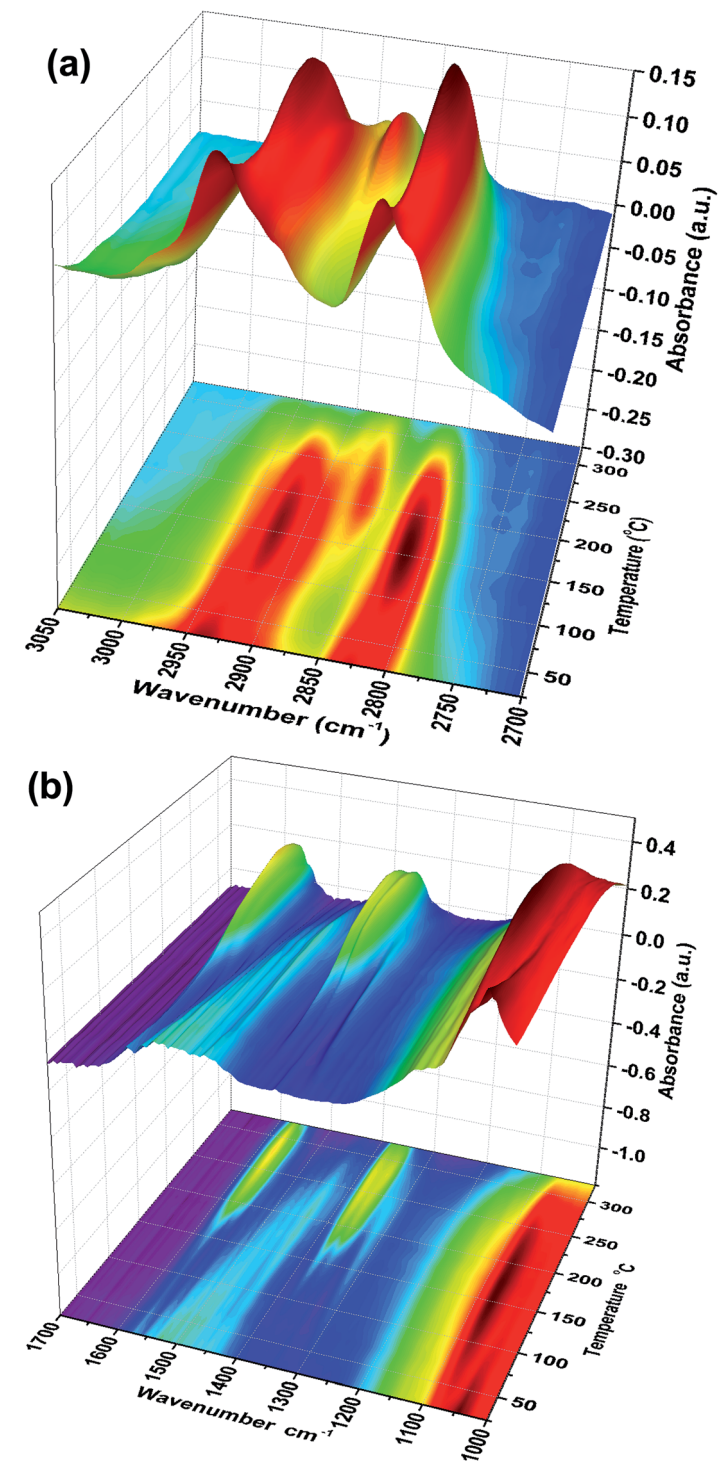


Fig. 2 Stacked TPD-RFTR spectra under He, in the (a) 2700–3050  $\text{cm}^{-1}$  and (b) 1000–1700  $\text{cm}^{-1}$  range.



**Table 1** Assignments for the bands observed in the DRIFTS experiments, <sup>a</sup> bands observed above ~150 °C, <sup>b</sup> bands observed above 175 °C

Assignment	Methoxy <sup>9</sup> (cm <sup>-1</sup> )	Methanol <sup>9</sup> (cm <sup>-1</sup> )	Formate <sup>10</sup> (cm <sup>-1</sup> )	This work, above 100 °C, (cm <sup>-1</sup> )	
				TPD	TPO
$\nu_{\text{as}}(\text{COO}) + \delta(\text{CH})$			2960	2960 <sup>b</sup>	2964 <sup>a</sup>
$\nu_{\text{s}}(\text{CH})$	2898	2925	2880	2922, 2895, 2866 <sup>b</sup>	2923, 2895, 2864 <sup>a</sup>
$2\delta(\text{CH}_3)$	2805	2824		2816	2818, 2808
$\nu_{\text{s}}(\text{COO}) + \delta(\text{CH})$			2730	2734 <sup>b</sup>	2734 <sup>a</sup>
$\nu_{\text{as}}(\text{COO})$			1565	1569 <sup>b</sup>	1571 <sup>a</sup>
$\delta(\text{CH})$	$\delta_{\text{as}}(\text{CH})$ 1460, $\delta_{\text{s}}(\text{CH})$ 1439		1379	1377 <sup>b</sup>	1376 <sup>a</sup>
$\nu_{\text{s}}(\text{COO})$			1358	1358 <sup>b</sup>	1355 <sup>a</sup>
$\nu(\text{CO})$ <sup>11</sup>	1070	1036		1073	1070



Fig. 4 shows a similar TPD experiment, but this time it is run in a flow of O<sub>2</sub>/He, effectively TPO, temperature-programmed oxidation. The results are rather revealing and different from those in Fig. 1. Here we still have the major CO<sub>2</sub> evolution at ~300 °C, but there is little hydrogen coincident with it. Instead the hydrogen evolution is now shifted down to ~200 °C and appears to be

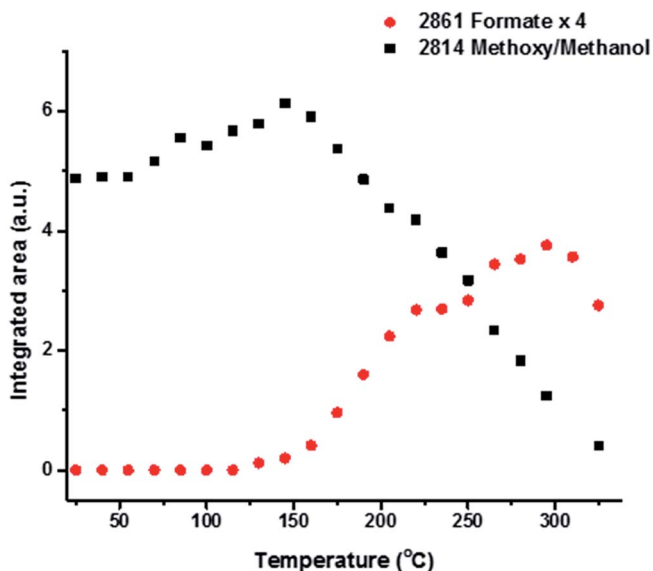


**Fig. 3** Integrated intensities of the main bands due to methoxy and formate species on the iron oxide surface as a function of temperature during TPD of methanol under a flow of He.



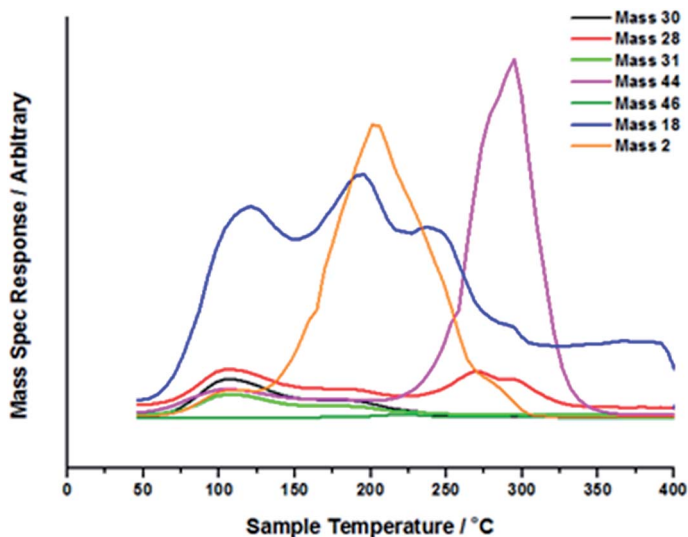


Fig. 4 TPD profile of  $\text{Fe}_2\text{O}_3$  under a  $8\text{ °C min}^{-1}$  ramp in a flow of 10%  $\text{O}_2/\text{He}$  after methanol adsorption.

independent of  $\text{CO}_2$  evolution. There is also water desorbing in a rather broad band of peaks from  $\sim 100\text{--}300\text{ °C}$ , and a small  $\text{CO}$  evolution at about  $270\text{ °C}$  (mass 28 for  $\text{CO}$  is a cracking fragment of mass 44 for  $\text{CO}_2$ , but the lineshape of the two here is different). The IR data are shown in Fig. 5 and 6. In Fig. 6 the same main bands are seen as in Fig. 2, that is, the formate and the methoxy, but now the ratio of these two IR bands is different, with much more formate formed. Further, the main hydrogen evolution appears to relate to the methoxy decomposition: the highest rate of loss of methoxy in IR (Fig. 6) is at about  $190\text{ °C}$ , corresponding with the peak in the TPD. The methoxy peak is lost in IR by about  $250\text{ °C}$ , corresponding with the end of the main hydrogen desorption. Similarly the formate band in IR is maximised at about the same temperature ( $\sim 300\text{ °C}$ ) as the  $\text{CO}_2$  desorption.

Experiments were carried out with the pulsed flow reactor described in the experimental section, and the data are displayed in Fig. 7, as a plot of the integrals of products as a function of temperature. In this situation, where only methanol is present during pulses into the  $\text{He}$  flow, the product profile is broadly similar to the results of the transient TPD experiments above. Here there is some hydrogen production, but the products are predominantly those of combustion, with methanol conversion beginning at around  $160\text{ °C}$ , reaching 50% conversion by  $\sim 220\text{ °C}$  and 100% by  $\sim 260\text{ °C}$ . The first product is that of dehydration, dimethyl ether (46 amu), together with water. This occurs at low conversion, maximising at  $200\text{ °C}$ , but with high selectivity at these low conversions. This is followed by  $\text{CO}$  and  $\text{H}_2$  seen between  $220\text{--}300\text{ °C}$  (28 and 2 amu peaks at that point), and with  $\text{CO}_2$  and  $\text{H}_2\text{O}$  becoming dominant above  $250\text{ °C}$ . At the highest temperatures there is also some methane production, beginning at about  $350\text{ °C}$  (increase in 16 amu, while carbon dioxide decreases). Clearly, since there is significant water production here, we must be reducing the iron oxide catalyst and labilising oxygen from subsurface regions. In the TPD experiment of Fig. 1 this does not



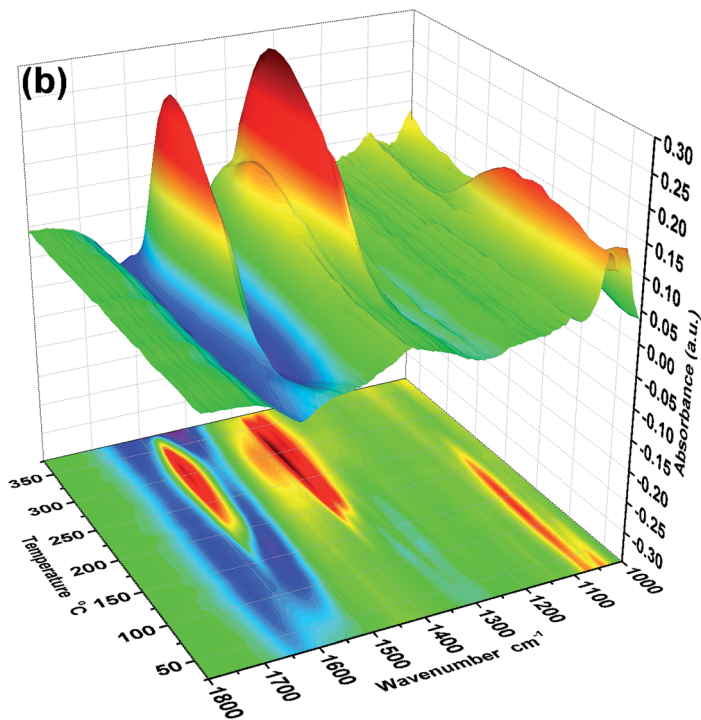
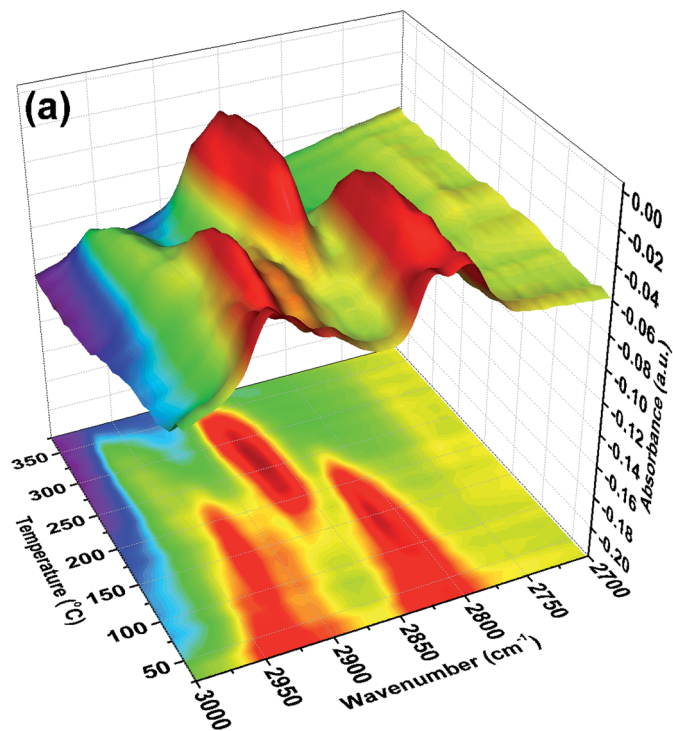


Fig. 5 Stacked TPDRIFTS under 10% O<sub>2</sub>/He spectra in the (a) 2700–3000 cm<sup>-1</sup> and (b) 1000–1800 cm<sup>-1</sup> range.



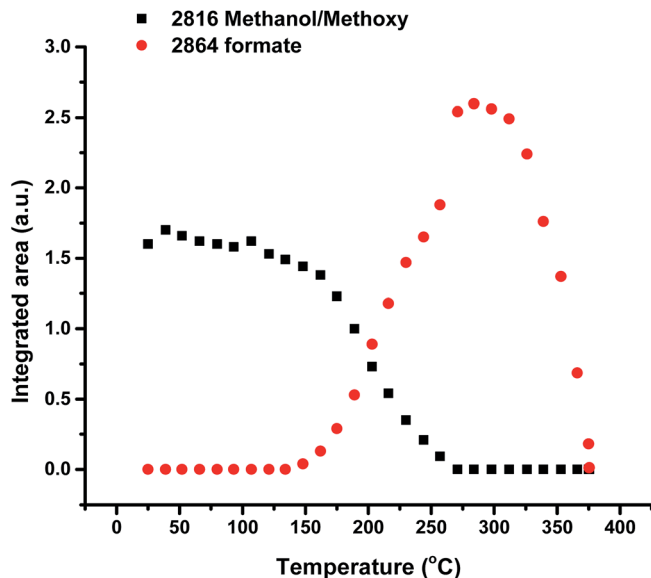


Fig. 6 Integrated intensities of the main bands due to methoxy and formate species on the iron oxide surface as a function of temperature during TPD of methanol under a flow of 10% O<sub>2</sub>/He.

occur, but, of course, methanol is not present in the gas phase during those experiments, and is only adsorbed on the surface layer.

If the same experiment is carried out in aerobic conditions, in a flow of 10% O<sub>2</sub>/He (Fig. 8), the results are broadly similar, but conversion is shifted to somewhat lower temperature and there is reduced hydrogen production.

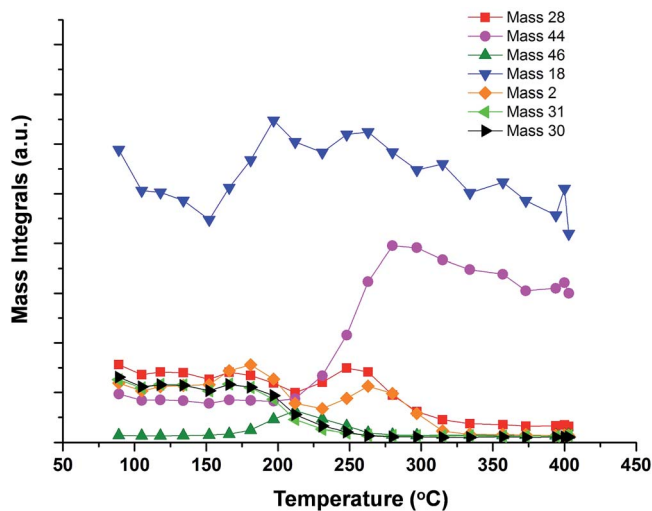


Fig. 7 TPR (temperature-programmed pulsed reaction) profiles for methanol pulses into a flow of He.



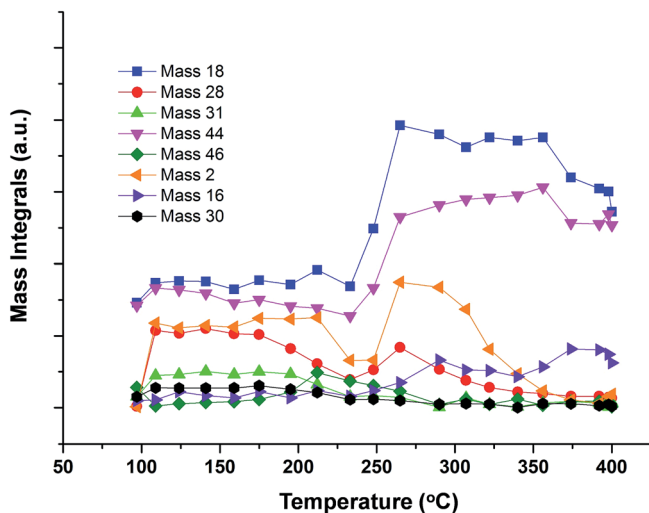


Fig. 8 TPR (temperature-programmed pulsed reaction) profiles for methanol pulses into a flow of 10% O<sub>2</sub>/He.

Clearly then, the following series of reactions takes place on the haemetite surface.



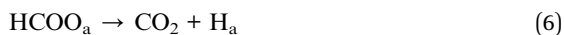
where the subscript a refers to adsorbed species and S is an adsorption site.



The reason for writing DME production in this form, that is, the reaction of surface methoxy with gas phase methanol, is that (i) DME production ceases in Fig. 7 when methanol conversion is very high (*i.e.* little methanol in the gas phase) and (ii) we see no DME in the TPD experiments, where there is no gas phase methanol dosed during the temperature ramp. The other reactions are:



Here O<sub>sl</sub> refers to lattice oxygen in the iron oxide, but which is at the surface and so available for reaction (and intrinsically different from lattice oxygen in the bulk). It is formed from the IR experiments during the temperature ramp above 150 °C. The formate can then decompose as follows:



and the liberated hydrogen then has two possible routes to loss from the surface, recombination to gas phase hydrogen or reaction with surface hydroxyls to give water.

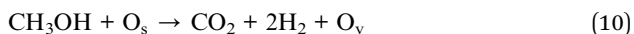




Finally it also appears that once the surface has become sufficiently reduced, methane can be evolved into the gas phase, presumably by a deoxygenation reaction with anion vacancies at the surface:



From these various data we can get an idea of the reaction kinetics involved here. If we first examine the formate decomposition, step 6, we can analyse the leading edge in Fig. 1 to give an activation energy of  $128 \text{ kJ mol}^{-1}$ . We can obtain the formation kinetics for the formate from the curve in Fig. 6 between 10 and 20 minutes reaction time ( $\sim 120\text{--}220 \text{ }^\circ\text{C}$ ) before formate decomposition occurs, and that value is  $60 \text{ kJ mol}^{-1}$ . For the anaerobic experiments the surface ends up in a reduced state, since  $\text{CO}_2$  is a product, so, at least in the surface region, the overall reaction in the absence of gas phase oxygen is



and clearly the dominant process in the TPD of Fig. 1 is hydrogen evolution, also seen in Fig. 4. However, in these cases methanol was not present in the gas phase during the TPD. Fig. 7 and 8 also show that when methanol is present in the gas phase, then water production dominates above  $300 \text{ }^\circ\text{C}$ , though some hydrogen is produced at intermediate temperatures. So  $\text{H}_2$  can apparently reduce the sample under these conditions:



We have gone on to make model catalysts related to industrial formaldehyde synthesis catalysts, which are iron molybdates.<sup>6</sup> These convert methanol by selective oxidation, with high selectivity. We have deposited monolayers of Mo on the surface of iron oxide, because then otherwise bulk spectroscopic techniques (such as XAS<sup>12,13</sup>) can be used to give surface information, if they are sensitive to Mo. When Mo is deposited onto the surface of the iron oxide there is a complete change of behaviour from that described above. TPD results reported in ref. 13 show that the main product is now formaldehyde, with no  $\text{CO}_2$  produced. Similarly, reactor results (not shown, but see ref. 6 and 8) show high selectivity to formaldehyde in the temperature range  $200$  to  $350 \text{ }^\circ\text{C}$ . This in itself shows that once Mo is deposited onto the surface it remains there after calcination, and repeated TPD experiments are reproducible. Spectroscopy and electron microscopy confirm such surface stability.<sup>12,13</sup> The TPD alone implies that the methoxy species dominates the surface and that dehydrogenation of this species yields the formaldehyde. This is confirmed from TPDRIFTS studies, Fig. 9, which show only the presence of methoxy on the surface after the adsorption of methanol. This methoxy species is lost at approximately the same temperature as the formaldehyde peak appears in the TPD.<sup>13</sup> No conversion



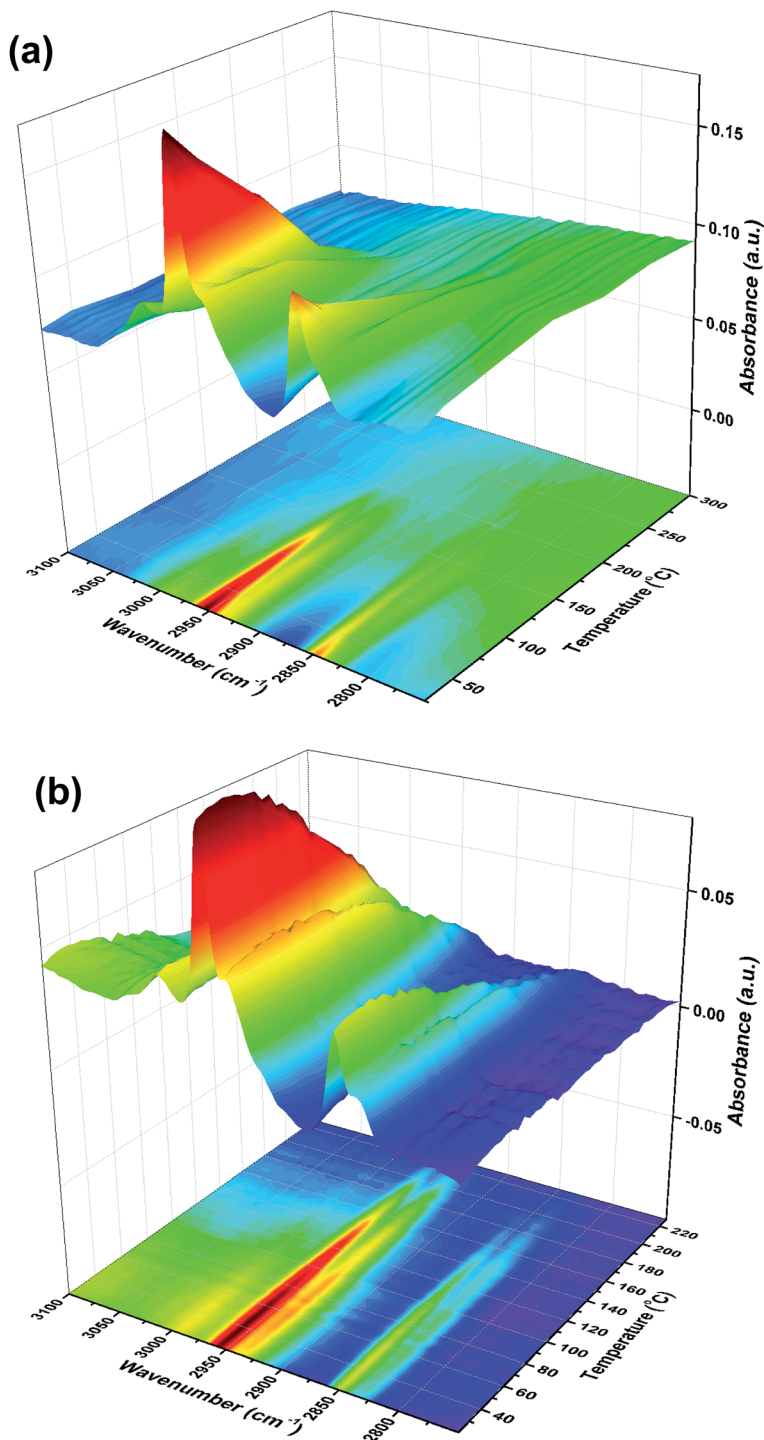


Fig. 9 Stacked TPDRIFTS under (a) He and (b) 10%  $\text{O}_2/\text{He}$  after adsorption of methanol on 6 monolayers of molybdena on  $\text{Fe}_2\text{O}_3$ .



to formate species is observed over these catalysts. Thus the presence of Mo appears to block step 5 above.

## Conclusions

Model catalysts of haematite and shell/core molybdena/haematite have been produced and their interaction with methanol examined. Haematite is shown to convert methanol into adsorbed methoxy, which is then oxidised to formate, the intermediate to combustion. In contrast, when dosed with surface Mo, the material becomes very selective to formaldehyde production and the formate pathway is blocked. Such materials, then, can make very useful model catalysts for answering a number of questions about catalytic behaviour.

## Acknowledgements

The UK Catalysis Hub is kindly thanked for resources and support provided *via* our membership of the UK Catalysis Hub Consortium and funded by EPSRC (portfolio grants EP/K014706/1, EP/K014668/1, EP/K014854/1, EP/K014714/1, and EP/I019693/1) and to Diamond plc for support for a studentship to CB.

## References

- 1 C. Rhodes, G. J. Hutchings and A. M. Ward, *Catal. Today*, 1995, **23**, 43.
- 2 A. Y. Khodakov, W. Chu and P. Fongarland, *Chem. Rev.*, 2007, **107**, 1692.
- 3 N. Mimura and M. Saito, *Catal. Today*, 2000, **55**, 173.
- 4 I. D. Gonzalez-Jimenez, K. Cats, T. Davidian, M. Ruitenbeek, F. Meirer, Y. Liu, J. Nelson, J. C. Andrews, P. Pianetta, F. M. F. de Groot and B. M. Weckhuysen, *Angew. Chem., Int. Ed.*, 2012, **51**, 11986.
- 5 A. P. V. Soares, M. F. Portela and A. Kiennemann, *Catal. Rev.*, 2005, **47**, 125.
- 6 M. Bowker, R. Holroyd, A. Elliott, A. Alouche, C. Entwistle and A. Toerncrona, *Catal. Lett.*, 2002, **83**, 165.
- 7 M. P. House, A. F. Carley, R. Echeverria-Valda and M. Bowker, *J. Phys. Chem. C*, 2008, **112**, 4333.
- 8 M. Bowker, C. Brookes, A. F. Carley, M. P. House, M. Kosif, G. Sankar, I. Wawata, P. P. Wells and P. Yaseneva, *Phys. Chem. Chem. Phys.*, 2013, **15**, 12056.
- 9 G. Busca, J. Lamotte, J.-C. Lavalley and V. Lorenzelli, *J. Am. Chem. Soc.*, 1987, **109**, 5197.
- 10 L. J. Burcham, L. E. Briand and I. E. Wachs, *Langmuir*, 2001, **17**, 6175.
- 11 A. Glisenti, G. Favero and G. Granozzi, *J. Chem. Soc., Faraday Trans.*, 1998, **94**, 173.
- 12 C. Brookes, P. P. Wells, G. Cibir, N. Dimitratos, W. Jones and M. Bowker, *ACS Catal.*, 2014, **4**, 243.
- 13 C. Brookes, P. P. Wells, N. Dimitratos, W. Jones, E. K. Gibson, D. J. Morgan, G. Cibir, C. Nicklin, D. Mora-Fonz, D. O. Scanlon, C. R. A. Catlow and M. Bowker, *J. Phys. Chem. C*, 2014, **118**, 26155.

